THE JOURNAL OF PHYSICAL CHEMISTRY Letters

Letter

pubs.acs.org/JPCL

Absolute Photoluminescence Quantum Yield Measurement in a Complex Nanoscopic System with Multiple Overlapping States

Narain Karedla, Jörg Enderlein,* Ingo Gregor, and Alexey I. Chizhik*

III. Institute of Physics, Georg August University, 37077 Göttingen, Germany

Supporting Information

ABSTRACT: Using a metal nanocavity, we measure absolute values of the photoluminescence quantum yield in a mixture of different types of chromophores (dye molecules and semiconductor nanocrystals). We show that measurements can be performed in an attoliter volume, both in liquid and solid phases, even if both types of chromophores absorb and emit light in the same spectral range. The method is based on recording photoluminescence decay curves of the chromophore mixture as a function of the cavity length. Changing the distance between the cavity mirrors modifies the local density of states of the electromagnetic field and thus, the radiative transition rate of the enclosed emitters. By extracting individual decay components, corresponding to the different types of the emitters, we determine their quantum yield values separately and simultaneously. The nanocavity-based method opens up new perspectives for studying quantum emitters in complex photophysical systems, for instance, multichromophoric thin films, fluorescent proteins, or dyes incorporated into a lipid bilayer.

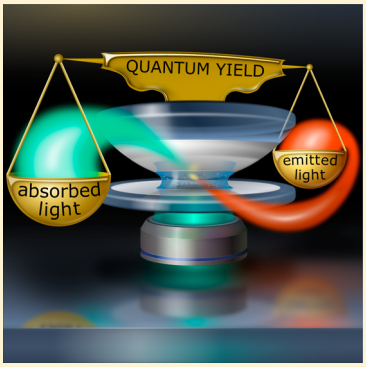

SECTION: Spectroscopy, Photochemistry, and Excited States

The photoluminescence quantum yield (QY), which describes the probability that a chromophore emits a photon upon its return from the excited to the ground state, plays a key role in numerous applications that involve photoluminescence, energy transfer, photovoltaics, or lasing.[1−5]

Recent progress in nanotechnology allows for confining complex photophysical systems within nanometric volumes, opening up new perspectives in optoelectronics. The photoluminescence QY, characterizing the fundamental photo-optical properties of such systems, is strongly dependent on the local physicochemical environment.[6] Therefore, an accurate measurement of the QY is essential for studying complex nanoscopic, possibly multichromophoric systems.[7,8] In the past, it has been very challenging if not impossible to measure QY values precisely and absolutely in nanometric volumes and at nano- to micromolar concentrations. Recently, we introduced a nanocavity-based method of determining the photoluminescence QY, which requires only a few microliters of low-concentrated chromophore solution,[9,10] and which is applicable even to single emitters.[6]

The core idea of the nanocavity-based method is to measure the change of the photoluminescence lifetime of quantum emitters inside an optical resonator with subwavelength spacing as a function of the distance between the metal cavity mirrors. A metal mirror changes the local density of the electromagnetic field modes.[11] As a result, chromophores located close to a metal surface[12,13] or between the mirrors of a metal nanocavity,[14−19] change their radiative transition rate, which depends on the emitter's transition dipole moment and the local density of modes of the electromagnetic field.[20] On the other hand, the photoluminescence QY of a chromophore can be represented as the ratio of its radiative to the nonradiative rate

$$\Phi = k_{rad}/(k_{rad} + k_{nr}) \quad (1)$$

Modeling the cavity-induced modulation of k_{rad} as a function of cavity length, and knowing the full excited-to-ground state transition rate $k_{rad} + k_{nr}$ as determined in a lifetime measurement, one can extract an absolute value of a chromophore's QY. The detailed description of the complete and quantitative theoretical model for the data evaluation, which takes into account the electric field distribution within the cavity as generated by the focused laser beam, the electromagnetic coupling of the dipole emission to the cavity, and the molecule detection function can be found elsewhere.[10] It has been recently shown that the nanocavity-based method allows for measuring even the QY of several types of chromophores emitting at different wavelengths but having strongly overlapping absorption spectra in a mixture.[21]

Here, we show that the nanocavity-based method allows for extracting QY values of two different types of chromophores (dye molecules and semiconductor nanocrystals, abbreviated later as NCs) with completely overlapping absorption and emission spectra, which is impossible to do by any other existing technique. Using a metal subwavelength nanocavity, we perform the measurements both in a low-concentrated solution and a thin solid chromphore-doped polymer film (Figure 1a−d). As already pointed out, the idea is to change the distance

Received: January 31, 2014
Accepted: March 18, 2014

   dx.doi.org/10.1021/jz500221t | J. Phys. Chem. Lett. 2014, 5, 1198−1202

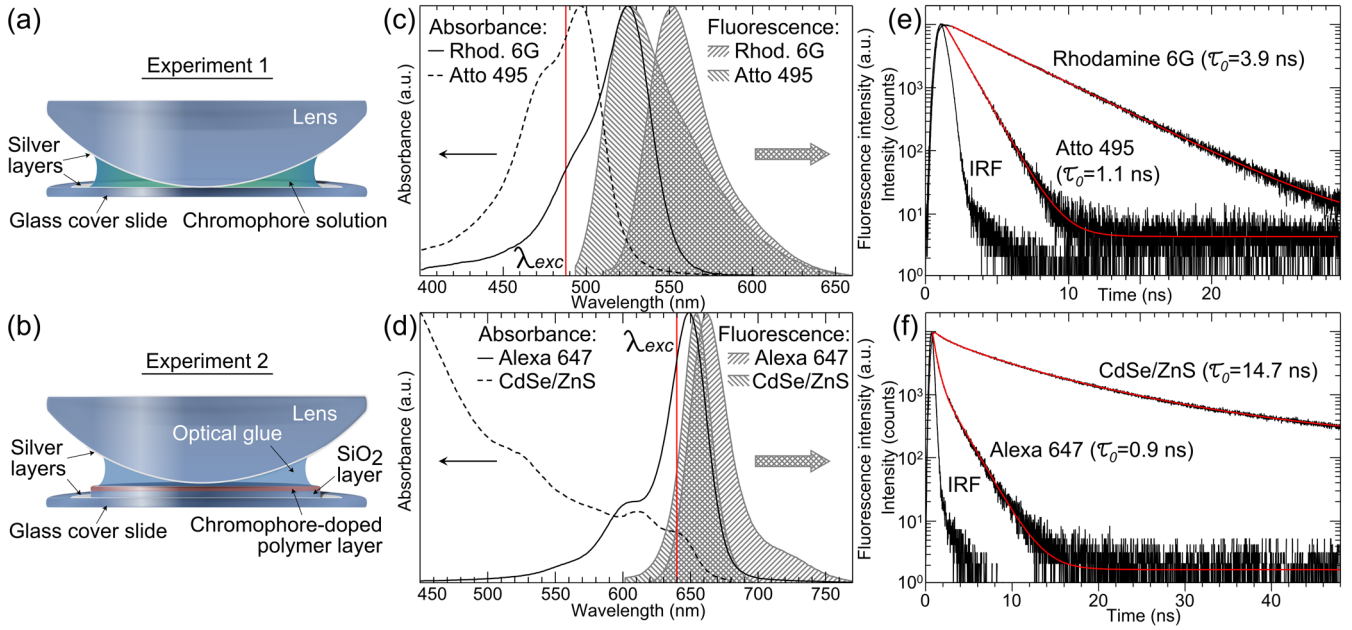

Figure 1. (a,b) Scheme of the cavity cross-section. The nanocavity consists of two silver layers, deposited on two glass surfaces. The upper silver layer is sputtered on the surface of a plan-convex lens, which allows one to tune the cavity length by moving the laser focus laterally. It should be noted that within the diffraction limited focal spot of the objective, the curvature of the upper surface is negligible, and the cavity can be considered to be a plane-parallel resonator. Between the cavity mirrors were placed a droplet of a mixture of rhodamine 6G and Atto 495 in water (a) and a thin solid polymer film doped with Alexa 647 and CdSe/ZnS NCs (b). (c,d) Room-temperature photoluminescence (shaded area) and absorption spectra (solid and dashed curves) of rhodamine 6G and Atto 495 in aqueous solution (c) and Alexa 647 and CdSe/ZnS NCs in a thin solid polymer film (d) on a clean glass cover slide. The vertical red line indicates the excitation wavelength of 488 nm (c) and 640 nm (d). (e) The black solid curves represent the photoluminescence decay curves of rhodamine 6G and Atto 495, and the instrument response function (IRF). The red curves show the fit with a monoexponential decay function to the experimental data yielding photoluminescence lifetime values 3.9 and 1.1 ns for rhodamine 6G and Atto 495, respectively. (f) The black solid curves show the photoluminescence decay curves of Alexa 647 and CdSe/ZnS NCs, and the IRF. The red curves show the fit with a multiexponential decay model, from which the average excited-state lifetime was calculated.

between the cavity mirrors, which modifies the local density of modes of the electromagnetic field and thus the radiative transition rate of the embedded emitters. Sufficient difference between the excited state lifetimes of the selected types of chromophores (Figure 1e,f) allows us to separate the decay components corresponding to different types of chromophores from the total signal. By fitting the resulting dependency of the photoluminescence lifetime on cavity length, we extract the QY values for each type of the chromophores. The measurement volume is determined by the lateral dimensions of the diffraction-limited focal spot, which shows the applicability of the method to nanoscopic system both in liquid and solid phase. The results presented here show that the nanocavity-based technique can be applied to the systems with complex quantum structure exhibiting multiple excited-to-ground-state transitions, as long as these transitions can be distinguished by their separated transition rates. This opens up new perspectives for studying multichromophoric thin films, fluorescent proteins, dyes incorporated into a lipid bilayer, etc.

Figure 1a,b displays a schematic of the nanocavity, which consists of two silver mirrors with subwavelength spacing, which were used for experiments 1 and 2, respectively. The bottom silver mirror (30 nm thick) was prepared by vapor deposition of silver onto a commercially available and cleaned microscope glass coverslide (thickness 170 μm) using an electron beam source (Laybold Univex 350) under high-vacuum conditions ($\sim 10^{-6}$ mbar). The top silver mirror (80 nm thick) was prepared by vapor deposition of silver onto the surface of a plan-convex lens (focal length of 150 mm) under the same conditions. Film thickness was monitored during vapor deposition using an oscillating quartz unit and verified by atomic force microscopy measurements. The spherical shape of the upper mirror allowed us to reversibly tune the cavity length by moving the laser focus laterally away or toward the cavity center. It should be noted that across the diffraction-limited laser focus, the cavity can be considered to be a plane-parallel resonator.[22] At each measurement position, the cavity length was determined by measuring the white light transmission spectrum using a spectrograph (Andor SR 303i) and a CCD camera (Andor iXon DU897 BV), and by fitting the spectra using standard Fresnel theory of transmission through a stack of plane-parallel layers, where the cavity length was the only free fit parameter.

A schematic of the home-built confocal microscope is shown in Figure 2. Photoluminescence lifetime measurements were performed with a home-built confocal microscope equipped with an objective lens of high numerical aperture (Apo N, 60 × /1.49 NA oil immersion, Olympus). A white light laser system (Fianium SC400−4−20) with a tunable filter (AOTFnC-400.650-TN) served as the excitation source. The light was reflected by a dichroic mirror (Semrock BrightLine FF484-FDi01 in experiment 1 and Di01-R405/488/561/635 in experiment 2) toward the objective, and backscattered excitation light was blocked with a long pass filter (Semrock EdgeBasic BLP01-488R in experiment 1 and BLP01-635R in experiment 2). Collected photoluminescence was focused onto the active area of an avalanche photo diode (PicoQuant τ-SPAD). Data acquisition was accomplished with a multichannel picosecond event timer (PicoQuant HydraHarp 400). Photon arrival times were histogrammed (bin width of 16 ps) for

dx.doi.org/10.1021/jz500221t | J. Phys. Chem. Lett. 2014, 5, 1198−1202

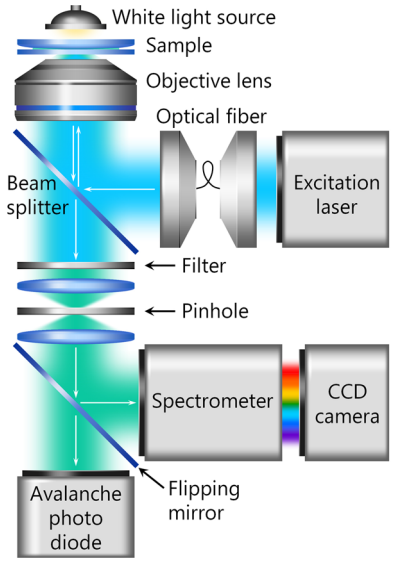

Figure 2. Scheme of the experimental setup.

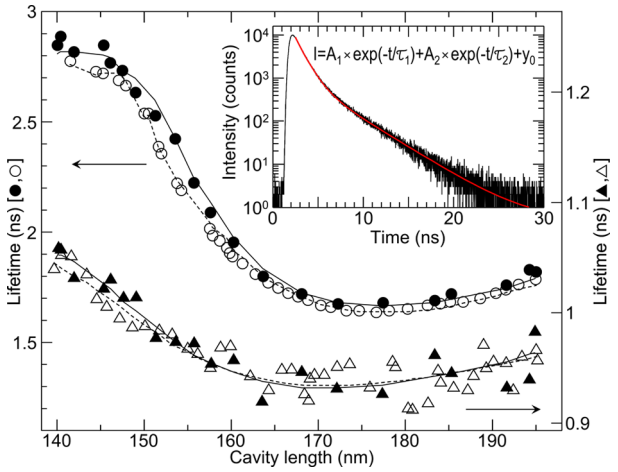

Figure 3. Measured photoluminescence lifetime as a function of the cavity length: solid circles - rhodamine 6G in a mixture with Atto 495 (left scale); open circles - rhodamine 6G in pure water (left scale); solid triangles - Atto 495 in a mixture with rhodamine 6G (right scale); open triangles - Atto 495 in pure water (right scale). Solid and dashed curves are the theoretical fits to the values measured in a mixture of dyes and in separate solutions, respectively. The fit results are summarized in Table 1. The inset shows an exemplary decay curve measured on a mixture of rhodamine 6G and Atto 495 inside the cavity. The red curve represents the fit with a biexponential decay function.

obtaining photoluminescence decay curves, and all curves were recorded until reaching 10^4 counts at the maximum. Rhodamine 6G molecules purchased from Sigma Aldrich, Atto 495 purchased from Atto-Tec, Alexa 647 and CdSe/ZnS NCs were purchased from Invitrogen. The ratio of concentrations of rhodamine 6G and Atto 495 in experiment 1 and Alexa 647 and CdSe/ZnS NCs in experiment 2 was adjusted to achieve nearly equal intensities of the photoluminescence decay curves for better separation of the two components. As the measurement was done at submicromolar concentration, one can neglect any modification of the QY due to interaction between the molecules. Measurements were performed in a range of white light transmission maxima between 500 and 720 nm, which overlaps with the emission spectra of the selected chromophores (Figure 1b,c). The absorption spectra were measured using a spectrophotometer (Jasco V-650).

In experiment 1 we measured the QY of rhodamine 6G and Atto 495 in aqueous solution in a mixture (Figure 1c). After placing a droplet of dye solution inside the nanocavity (Figure 1a), we recorded the photoluminescence decay curves of the chromophore mixture as a function of cavity length. Every curve was fitted with a biexponential decay function giving the decay times for each of the two dyes at every measured cavity length (see inset in Figure 3). The fitted decay times for rhodamine 6G (solid circles) and Atto 495 (solid triangles) as a function of cavity length are shown in Figure 3. Note that the scale at the right side of the figure, which corresponds to the lifetime values of Atto 495, is rescaled by a factor of 5 with respect to the left one. The black solid lines are the fits of the experimental curves with a theoretical model of the relation between cavity length and lifetime, where the only free parameters were the free-space lifetime τ_0 and the photoluminescence QY value Φ.

The obtained values of the free space lifetime for rhodamine 6G (4.0 ns) and Atto 495 (1.2 ns) are in good agreement with the lifetime values of these chromophores measured in separate solutions on a glass cover slide (3.9 and 1.1 ns for rhodamine 6G and Atto 495, respectively; see Figure 1e). The deviation between the calculated and directly measured free space lifetime values originates from the error of fitting of the photoluminescence decay curves, which is typically on the order of 0.1 ns for the selected signal intensity. The measured photoluminescence QY values are 0.89 for rhodamine 6G and 0.15 for Atto 495. To verify the accuracy of the obtained QY values as extracted from the lifetime measurements on the dye mixture, we determined the QY values of rhodamine 6G and Atto 495 separately using the nanocavity method under identical conditions. The measured lifetime values as a function of cavity length are shown in Figure 3, where open circles refer to rhodamine 6G and triangles to Atto 495. The theoretical fits of the lifetime values as measured separately in pure solutions of one dye are shown as dashed lines. They yield QY values of 0.95 for rhodamine 6G, and of 0.13 for Atto 495.

In experiment 2 we determined the photoluminescence QY of Alexa 647 dye and CdSe/ZnS core−shell semiconductor NCs emitting at 655 nm. Both types of the chromophores were spin-coated in a mixture with polymer (PVA) on a SiO_2 spacer deposited on the bottom cavity mirror. As a result, both types of chromophores were immobilized in a thin (near 50 nm) polymer film. A droplet of the optical glue was placed between the cavity mirrors to match the refractive index. Because of the local variation of the chemical environment in a solid polymer film, the recorded decay curves exhibited a multiexponential behavior. To separate the decay components, corresponding to the emission from Alexa 647 and NCs, we employed the following fitting algorithm for the total decay curves recorded at every cavity length. As the free space lifetimes of Alexa 647 and selected semiconductor NCs differ by more than 1 order of magnitude (see Figure 1f), we first fitted the tail of the long component (emission from semiconductor NCs) starting from the time point, where the intensity of the short component drops to near 1% of its maximum, which is 7 ns in this case. Thus, we select the region of the total decay curve, where the contribution of the short component is negligible. The fitting within this region was done using the sum of the three monoexponential functions, which typically allows good

dx.doi.org/10.1021/jz500221t | J. Phys. Chem. Lett. 2014, 5, 1198−1202

agreement with the experimental data. By extrapolating the obtained fit to the first 7 ns, we obtained the full long component. The obtained curve was subtracted from the initial decay curve, which resulted in a pure short component, corresponding to the emission from Alexa 647. This algorithm allowed us to extract both multiexponential components of the total decay, taking into account their overlap within the time period where both types of the chromophores emit photons. Finally, the mean photoluminescence lifetime was obtained from the separated photoluminescence decay curves as:

$$\langle \tau \rangle = \int_0^\infty I(t)t \, dt / \int_0^\infty I(t) \, dt \quad (2)$$

where $I(t)$ is the photoluminescence intensity as a function of time after the excitation pulse. The obtained values of the photoluminescence lifetimes for CdSe/ZnS NCs (solid circles) and Alexa 647 (solid triangles) as a function of cavity length are shown in Figure 4. Note that the scale at the right side of the figure is rescaled by a factor of 10 with respect to the left one. The black solid lines are the fits of the experimental curves with a theoretical model of the relation between cavity length and lifetime, where the free parameters were the free space lifetime τ_0 and the photoluminescence QY value Φ. The obtained values of the free space lifetime for Alexa 647 (0.8 ns) and CdSe/ZnS NCs (13.6 ns) demonstrate a good agreement with the lifetime values of these chromophores measured in separate thin films on a glass cover slide (0.9 and 14.7 ns for Alexa 647 and CdSe/ZnS NCs, respectively; see Figure 1f). The photoluminescence QY values (0.61 for CdSe/ZnS NCs and 0.29 for Alexa 647) are also in a good agreement with the QY values obtained from the chromophores separately under identical conditions (0.25 for Alexa 647 and 0.73 for CdSe/ZnS NCs).

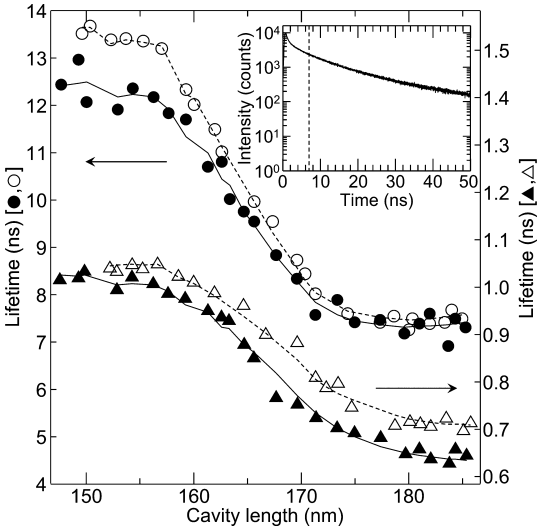

Figure 4. Measured photoluminescence lifetime as a function of the cavity length: solid circles - CdSe/ZnS NCs in a mixture with Alexa 647 (left scale); open circles - CdSe/ZnS NCs in a solid polymer film (left scale); solid triangles - Alexa 647 in a mixture with CdSe/ZnS (right scale); open triangles - Alexa 647 in a solid polymer film (right scale). Solid and dashed curves are the theoretical fits to the values measured in a mixture of chromophores and in separate samples, respectively. The fit results are summarized in Table 1. The inset shows an exemplary decay curve measured on a mixture of CdSe/ZnS and Alexa 647 inside the cavity. The dashed line separates the two areas, where the fitting of a long and short decay component was done (see main text for further details).

The results of fitting for both experiments are summarized in Table 1. The prominent agreement between the QY values as extracted from measurements in the mixture and in single-dye samples indicates that the nanocavity-based method allows for extracting separately QY values of emitters with overlapping emission and absorption spectra in a mixture, which is impossible to do by any other existing technique.

Table 1. Values of the Photoluminescence Quantum Yield Φ and the Free Space Lifetimes τ_0 of the Two Chromophores, When Measured in a Mixture (Superscript "mix"), and When Measured Separately (Superscript "sep")[a]

experiment	chromophore	Φ^{mix}	τ_0^{mix} (ns)	Φ^{sep}	τ_0^{sep} (ns)
experiment 1	Rhodamine 6G	0.89	4.0	0.95	4.1
	Atto 495	0.15	1.2	0.13	1.1
experiment 2	CdSe/ZnS NCs	0.61	13.6	0.73	15.2
	Alexa 647	0.29	0.8	0.25	0.9

[a]These values are obtained by fitting the data shown in Figures 3 and 4.

In order to determine the limitation of our technique in terms of the separation of different photoluminescence decay components, we calculated the separation probability for different pairs of the mono- and multiexponential decays. The results are shown in the Supporting Information. In particular, the separation of two monoexponential decay components can be done with at least 60% probability if the lifetimes differ at least by a factor of 2. In this case, the intensity ratio for the long and short components can vary within the range from 70/30 to 30/70. For the multiexponential decay curves, the separation can be done with the error not higher than 20% if the ratio of the lifetime values of the average long and short components is at least 5. The separation of the multiexponential components can be done both when the multiexponential character of the decay curves is induced by the inhomogeneous chemical environment (as in case of solid films) or related to intrinsic properties of an emitter itself.

The method works for samples both in liquid and solid phases, in a nanoscopic volume at low concentration of chromophores of various types. Thus, the nanocavity-based technique can be applied to a large number of systems with intrinsically multiexponential photoluminescence decay for studying individual deexcitation processes, as long as they can be distinguished by their separated transition rates. Among such systems are various fluorescent proteins,[23] amino acids,[1] aggregates in thin films[24] or multichromophoric systems.[25−27] Since the nanocavity-based method can be applied to any quantum emitter of interest, such as dye molecules, semiconductor NCs, carbon nanotubes, and so on, the possibility to measure QY values of chromophores incorporated into complex photophysical systems opens up new perspectives for studying the photophysics of complex nanometric systems.

■ ASSOCIATED CONTENT

Supporting Information

Analysis of the separable mono-exponential and multi-exponential decay curves. This material is available free of charge via the Internet at http://pubs.acs.org.

dx.doi.org/10.1021/jz500221t | J. Phys. Chem. Lett. 2014, 5, 1198−1202

AUTHOR INFORMATION

Corresponding Authors

*E-mail: enderlein@physik3.gwdg.de.
*E-mail: chizhik@physik3.gwdg.de.

Notes

The authors declare no competing financial interest.

ACKNOWLEDGMENTS

Financial support by the Deutsche Forschungsgemeinschaft is gratefully acknowledged (SFB 937, project A5). A.I.C. thanks the Alexander von Humboldt Foundation for financial support. N.K. is grateful to the Niedersächsisches Ministerium für Wissenschaft and Kultur for a MWK stipend.

REFERENCES

(1) Lakowicz, J. R. *Principles of Fluorescence Spectroscopy*, 3rd ed.; Springer: New York, 2006.
(2) Yorulmaz, M.; Khatua, S.; Zijlstra, P.; Gaiduk, A.; Orrit, M. Luminescence Quantum Yield of Single Gold Nanorods. *Nano Lett.* **2012**, *12*, 4385−4391.
(3) Piao, Y.; Meany, B.; Powell, L. R.; Valley, N.; Kwon, H.; Schatz, G. C.; Wang, Y. Brightening of Carbon Nanotube Photoluminescence through the Incorporation of sp^3 Defects. *Nat. Chem.* **2013**, *5*, 840−845.
(4) Zhao, J.; Chen, O.; Strasfeld, D. B.; Bawendi, M. G. Biexciton Quantum Yield Heterogeneities in Single CdSe (CdS) Core (Shell) Nanocrystals and Its Correlation to Exciton Blinking. *Nano Lett.* **2012**, *12*, 4477−4483.
(5) Hoy, J.; Morrison, P. J.; Steinberg, L. K.; Buhro, W. E.; Loomis, R. A. Excitation Energy Dependence of the Photoluminescence Quantum Yields of Core and Core/Shell Quantum Dots. *J. Phys. Chem. Lett.* **2013**, *4*, 2053−2060.
(6) Chizhik, A. I.; Chizhik, A. M.; Khoptyar, D.; Bär, S.; Meixner, A. J.; Enderlein, J. Probing the Radiative Transition of Single Molecules with a Tunable Microresonator. *Nano Lett.* **2011**, *11*, 1700−1703.
(7) Ando, Y.; Niwa, K.; Yamada, N.; Enomoto, T.; Irie, T.; Kubota, H.; Ohmiya, Y.; Akiyama, H. Firefly Bioluminescence Quantum Yield and Colour Change by pH-Sensitive Green Emission. *Nat. Photon.* **2008**, *2*, 44−47.
(8) Yang, R.; Garcia, A.; Korystov, D.; Mikhailovsky, A.; Bazan, G. C.; Nguyen, T.-Q. Control of Solution Aggregation, Solid State Fluorescence Quantum Yield, and Charge Transport in Cationic Conjugated Polyelectrolytes by Choice of Anion. *J. Am. Chem. Soc.* **2006**, *128*, 16532−16539.
(9) Chizhik, A. I.; Gregor, I.; Schleifenbaum, F.; Müller, C. B.; Röling, C.; Meixner, A. J.; Enderlein, J. Electrodynamic Coupling of Electric Dipole Emitters to a Fluctuating Mode Density within a Nanocavity. *Phys. Rev. Lett.* **2012**, *108*, 163002.
(10) Chizhik, A. I.; Gregor, I.; Ernst, B.; Enderlein, J. Nanocavity-Based Determination of Absolute Values of Photoluminescence Quantum Yields. *Chem. Phys. Chem.* **2013**, *14*, 505−513.
(11) Purcell, E. M. Spontaneous Emission Probabilities at Radio Frequencies. *Phys. Rev.* **1946**, *69*, 681.
(12) Drexhage, K. H. Interaction of Light with Monomolecular Dye Layers. *Prog. Opt.* **1974**, *12*, 163−232.
(13) Chizhik, A. I.; Rother, J.; Gregor, I.; Janshoff, A.; Enderlein, J. Metal-Induced Energy Transfer for Live Cell Nanoscopy. *Nat. Photon.* **2014**, *8*, 124−127.
(14) Vahala, K. J. Optical Microcavities. *Nature* **2003**, *424*, 839−846.
(15) Goy, P.; Raimond, J. M.; Gross, M.; Haroche, S. Observation of Cavity-Enhanced Single-Atom Spontaneous Emission. *Phys. Rev. Lett.* **1983**, *50*, 1903−1906.
(16) Kern, A. M.; Zhang, D.; Brecht, M.; Chizhik, A. I.; Failla, A. V.; Wackenhut, F.; Meixner, A. J. Enhanced Single-Molecule Spectroscopy in Highly Confined Optical Fields: from $\lambda/2$-Fabry-Pérot Resonators to Plasmonic Nano-Antennas. *Chem. Soc. Rev.* **2014**, *43*, 1263−1286.
(17) Chizhik, A.; Schleifenbaum, F.; Gutbrod, R.; Chizhik, A.; Khoptyar, D.; Meixner, A. J.; Enderlein, J. Tuning the Fluorescence Emission Spectra of a Single Molecule with a Variable Optical Subwavelength Metal Microcavity. *Phys. Rev. Lett.* **2009**, *102*, 073002.
(18) Chizhik, A. I.; Chizhik, A. M.; Kern, A. M.; Schmidt, T.; Potrick, K.; Huisken, F.; Meixner, A. J. Measurement of Vibrational Modes in Single SiO_2 Nanoparticles Using a Tunable Metal Resonator with Optical Subwavelength Dimensions. *Phys. Rev. Lett.* **2012**, *109*, 223902.
(19) Englund, D.; Shields, B.; Rivoire, K.; Hatami, F.; Vučković, J.; Park, H.; Lukin, M. D. Deterministic Coupling of a Single Nitrogen Vacancy Center to a Photonic Crystal Cavity. *Nano Lett.* **2010**, *10*, 3922−3926.
(20) Fermi, E. Quantum Theory of Radiation. *Rev. Mod. Phys.* **1932**, *4*, 87−132.
(21) Chizhik, A. I.; Gregor, I.; Enderlein, J. Quantum Yield Measurement in a Multicolor Chromophore Solution Using a Nanocavity. *Nano Lett.* **2013**, *13*, 1348−1351.
(22) Steiner, M.; Schleifenbaum, F.; Stupperich, C.; Failla, A. V.; Hartschuh, A.; Meixner, A. J. Microcavity-Controlled Single-Molecule Fluorescence. *Chem. Phys. Chem.* **2005**, *6*, 2190−2196.
(23) Habuchi, S.; Ando, R.; Dedecker, P.; Verheijen, W.; Mizuno, H.; Miyawaki, A.; Hofkens, J. Reversible Single-Molecule Photoswitching in the GFP-like Fluorescent Protein Dronpa. *Proc. Natl. Acad. Sci. U. S. A.* **2005**, *102*, 9511−9516.
(24) Gierschner, J.; Lüer, L.; Milián-Medina, B.; Oelkrug, D.; Egelhaaf, H.-J. Highly Emissive H-Aggregates or Aggregation-Induced Emission Quenching? The Photophysics of All-Trans *para*-Distyrylbenzene. *J. Phys. Chem. Lett.* **2013**, *4*, 2686−2697.
(25) Gao, X.; Cui, Y.; Levenson, R. M.; Chung, L. W. K.; Nie, S. In Vivo Cancer Targeting and Imaging with Semiconductor Quantum Dots. *Nat. Biotechnol.* **2004**, *22*, 969−976.
(26) Huynh, W. U.; Dittmer, J. J.; Alivisatos, A. P. Hybrid Nanorod−Polymer Solar Cells. *Science* **2002**, *295*, 2425−2427.
(27) Qian, F.; Gradečak, S.; Li, Y.; Wen, C-Y; Lieber, C. M. Core/Multishell Nanowire Heterostructures as Multicolor, High-Efficiency Light-Emitting Diodes. *Nano Lett.* **2005**, *5*, 2287−2291.